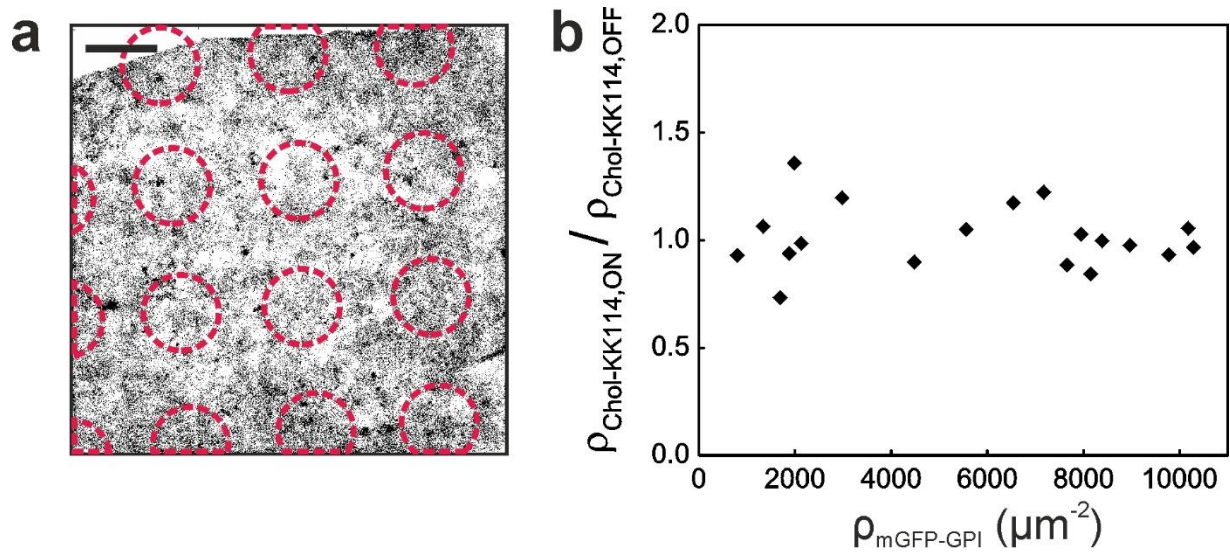


Supplementary Figures



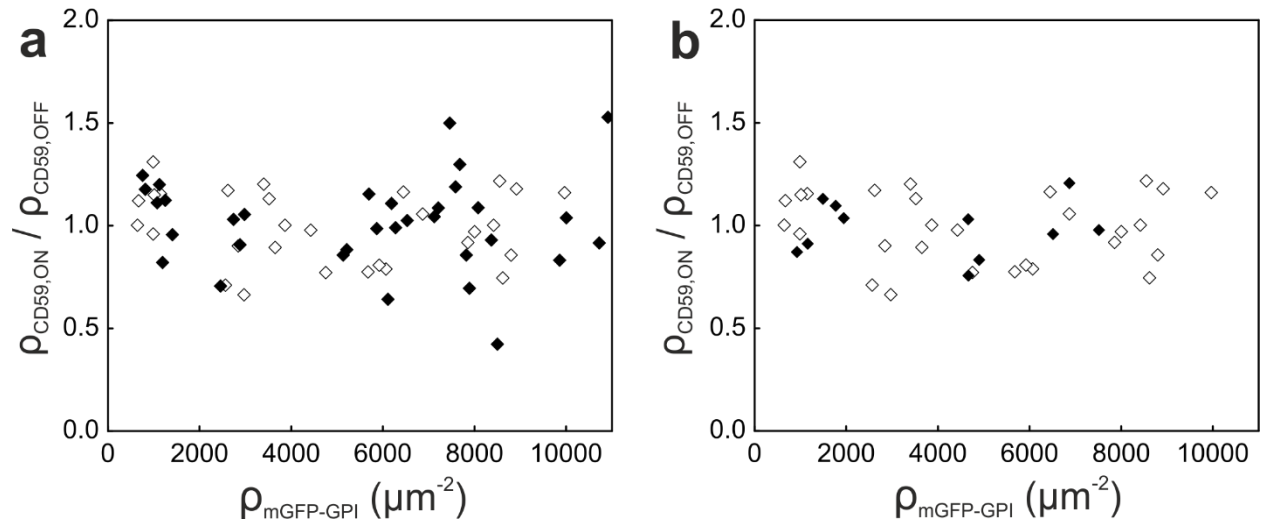
Supplementary Figure 1. Partitioning of Chol-KK114 in GPMVs.

Representative image of a giant plasma membrane vesicle derived from T24 cells labeled with the Ld-marker DiI (green, left) and Chol-KK114 (red, middle). Quantification of Chol-KK114 partitioning in 26 phase-separated GPMVs yielded $55 \pm 4\%$ Ld partitioning. Scale bar is 3 μm .



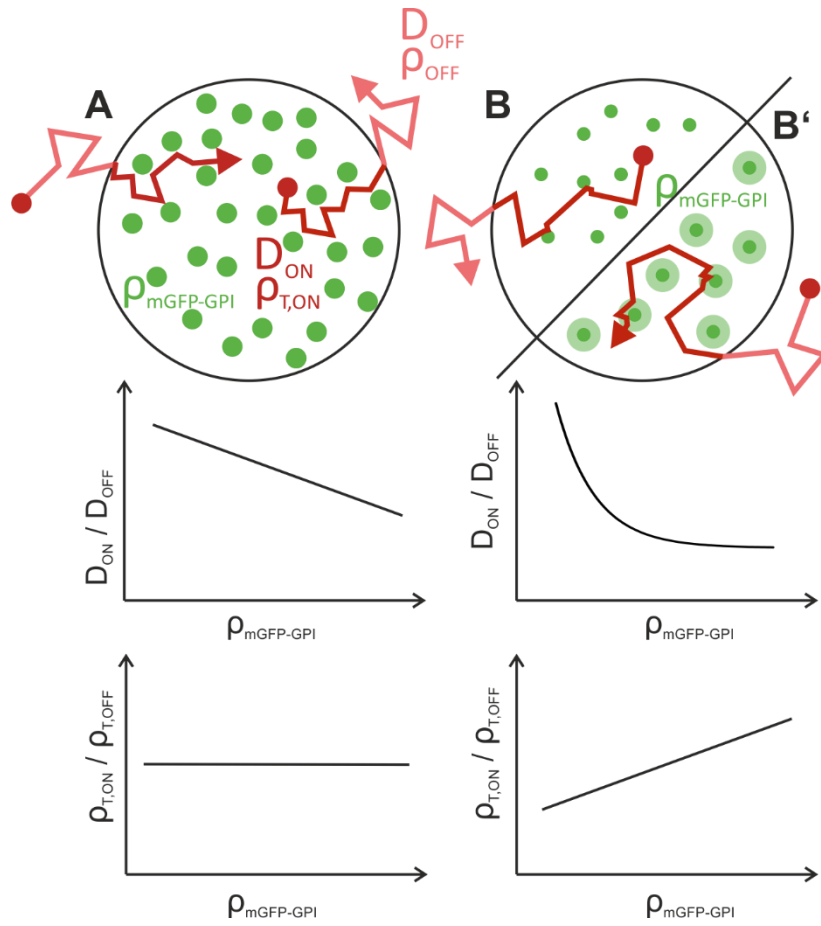
Supplementary Figure 2. Chol-KK114 is not recruited to mGFP-GPI areas.

a Chol-KK114 single molecule positions were recorded within a selected region of interest; the underlying mGFP-GPI patterns are shown as dotted red circles. Error bar is 3 μm . **b** The relative surface density of Chol-KK114, $\rho_{\text{Chol-KK114,ON}} / \rho_{\text{Chol-KK114,OFF}}$, is plotted as a function of the surface density of mGFP-GPI, $\rho_{\text{mGFP-GPI}}$, for 19 individual cells (four independent experiments).



Supplementary Figure 3. CD59 is homogeneously distributed between mGFP-GPI enriched (ON) and depleted (OFF) areas at 37°C and upon cholesterol depletion.

The relative surface density of CD59 $\rho_{\text{CD59,ON}} / \rho_{\text{CD59,OFF}}$ is plotted as a function of the surface density of mGFP-GPI upon cholesterol depletion **(b)** (N=34, six independent experiments) and at 37°C **(a)** (N=11, three independent experiments), respectively.



Supplementary Figure 4. Dependence of tracer diffusion and enrichment on the obstacle density is characteristic for the mode of interaction. *Scenario A:* mGFP-GPI acts as immobile repulsive obstacles to tracer diffusion: D_{ON}/D_{OFF} decreases with increasing $\rho_{mGFP-GPI}$ as described e.g. by Saxton¹. The tracer density in the accessible space between obstacles is increased owing to the inaccessible area covered by the obstacles, so that the average tracer density $\rho_{T,ON}/\rho_{T,OFF}$ remains unchanged. *Scenario B:* (Transient) binding of the tracer to immobile mGFP-GPI obstacles. D_{ON}/D_{OFF} decreases with increasing $\rho_{mGFP-GPI}$ due to increasing contribution of (transiently) immobilized tracers. Concomitantly, the tracer density $\rho_{T,ON}/\rho_{T,OFF}$ increases by the trapped fraction. The same effect would be produced by *Scenario B'*: Tracer partitioning into nanometer-sized domains around the obstacles.

Supplementary Table 1. Mean diffusion coefficients D ($\mu\text{m}^2/\text{s}$) and apparent diffusion coefficients D^* ($\mu\text{m}^2/\text{s}^\alpha$) from fits assuming anomalous diffusion. For this table, data corresponding to values of $d_{\text{mGFP-GPI}} < 15$ nm were pooled. Mean values \pm s.e.m. are shown. α is the anomalous diffusion exponent.

	D_{ON}	D_{OFF}	D^*_{ON}	D^*_{OFF}	α_{ON}	α_{OFF}
CD59						
23°C	0.21 \pm 0.02	0.29 \pm 0.02	0.12 \pm 0.01	0.19 \pm 0.01	0.89 \pm 0.01	0.92 \pm 0.01
23°C + CO	0.23 \pm 0.01	0.32 \pm 0.01	0.17 \pm 0.01	0.26 \pm 0.01	0.92 \pm 0.01	0.94 \pm 0.01
37°C	0.58 \pm 0.07	0.71 \pm 0.06	0.41 \pm 0.06	0.56 \pm 0.06	0.89 \pm 0.02	0.92 \pm 0.02
Chol-KK114						
23°C	0.31 \pm 0.03	0.34 \pm 0.03	0.25 \pm 0.02	0.27 \pm 0.02	0.93 \pm 0.01	0.91 \pm 0.01

Supplementary Notes

Supplementary Note 1. Comparison of our results with the model presented in Suzuki et al.²

Suzuki et al.² present a hierarchical model of plasma membrane organization where, as a first level of interactions, GPI-APs form reversible homodimers – but not heterodimers – through protein ectodomain interactions. Further, they propose that homodimers can coalesce to form hetero- and homo-GPI-AP oligomer rafts through lipid interactions. The first finding is in good agreement with the results of our study: we do not find enrichment of CD59 within mGFP-GPI enriched regions, ruling out any specific interactions between these GPI-APs. The latter statement, however, seems contradictory to our study: if indeed hetero-associates of GPI-APs could be formed via a lipid-mediated mechanism, we also should have found evidence for this interaction.

We think that the apparent discrepancy originates from the difficulty in precisely quantifying the lifetime of protein-protein interactions from single molecule co-diffusion experiments. Suzuki et al. were certainly aware of that and took care in accounting for it. However, specifically in this experiment, prolonged colocalization times may not only indicate the presence of an interaction between two homodimers, but can also reflect longer apparent co-diffusion times of two incidentally colocalized homodimers due to significantly slower diffusion. In fact, since the diffusion of an antibody-crosslinked CD59 is almost three times slower than that of a single CD59 molecule labeled with a Fab fragment³, a concomitant 3-fold increase in the co-diffusion times of antibody-crosslinked CD59 can be expected.

Supplementary References

1. Saxton, M.J. Lateral diffusion in an archipelago. Dependence on tracer size. *Biophys J* **64**, 1053-62 (1993).
2. Suzuki, K.G. et al. Transient GPI-anchored protein homodimers are units for raft organization and function. *Nat Chem Biol* **8**, 774-83 (2012).
3. Wieser, S., Moertelmaier, M., Fuertbauer, E., Stockinger, H. & Schütz, G.J. (Un)Confined Diffusion of CD59 in the Plasma Membrane Determined by High-Resolution Single Molecule Microscopy. *Biophys J* **92**, 3719-28 (2007).